Diabetic Neuroglial Changes in the Superficial and Deep Nonperfused Areas on Optical Coherence Tomography Angiography

Yoko Dodo, Tomoaki Murakami, Kiyoshi Suzuma, Shin Yoshitake, Tatsuya Yoshitake, Kenji Ishihara, Masahiro Fujimoto, Yuko Miwa, and Akitaka Tsujikawa

Department of Ophthalmology and Visual Sciences, Kyoto University Graduate School of Medicine, Kyoto, Japan

Correspondence: Tomoaki Murakami, Department of Ophthalmology and Visual Sciences, Kyoto University Graduate School of Medicine, 54 Shogoin-Kawaracho, Sakyo, Kyoto 606-8507, Japan; mutomo@kuhp.kyoto-u.ac.jp.

Submitted: May 2, 2017
Accepted: October 17, 2017

Citation: Dodo Y, Murakami T, Suzuma K, et al. Diabetic neuroglial changes in the superficial and deep nonperfused areas on optical coherence tomography angiography. *Invest Ophthalmol Vis Sci*. 2017;58:5870–5879. DOI: 10.1167/iovs.17-22156

Purpose. To evaluate the relationship between lamellar capillary nonperfusion on optical coherence tomography angiography (OCTA) images and neuroglial changes on structural optical coherence tomography (OCT) images in diabetic retinopathy (DR).

Methods. We retrospectively reviewed 101 consecutive eyes of 69 patients with DR. OCTA and OCT images within a 3 × 3-mm square centered on the fovea were acquired simultaneously. The nonperfused areas (NPAs) in the superficial capillary layer (sNPA) (from the nerve fiber layer [NFL] to the inner plexiform layer [IPL]), the deep layer (dNPA) (corresponding mainly to the inner nuclear layer [INL]), or both layers (bNPA) were measured individually along 10 transverse lines. The corresponding lamellar neuroglial changes also were evaluated on OCT images.

Results. The transverse lengths of the sNPA, dNPA, and bNPA were 2.34% (interquartile range, 0.81–5.55), 0.61% (0–1.99), and 5.96% (4.02–10.88), respectively. The length of the sNPA was correlated significantly with the lengths of no boundary between the NFL and ganglion cell layer (GCL)/IPL and the spots with inverted OCT reflectivity in the sNPA. The transverse length of the dNPA was associated with the length of cystoid spaces in the INL or Henle's fiber layer (HFL) in the dNPA. There was a significant correlation between the transverse lengths of the bNPA and no boundary between the NFL and GCL/IPL within the bNPA.

Conclusions. Systematic evaluation of the OCTA–OCT association showed structural changes in the neuroglial tissues corresponding to the lamellar NPAs and suggested the feasibility of layer-by-layer evaluation of the capillary nonperfusion in DR.

Keywords: diabetic retinopathy, capillary nonperfusion, optical coherence tomography angiography

Diabetic retinopathy (DR) often leads to severe visual loss in working-age individuals, although it remains to be determined how the pathophysiology in retinal vessels affects the neuroglial function and vice versa in DR.[1–3] The neurovascular unit sustains the retinal structure and function in healthy retinas, whereas diabetes-induced damage in the retinal vessels promotes edematous changes and impairs the exchange of gases, nutrients, and waste in the retinal parenchyma, which can be recognized clinically as diabetic macular edema (DME) and nonperfused areas (NPAs).

Recent advances in optical coherence tomography angiography (OCTA) technology have enabled an appreciation of the three-dimensional vascular architecture.[4–6] Histologic studies have reported that in healthy retinas the retinal vasculature resides mainly in the nerve fiber layer (NFL), ganglion cell layer (GCL), and the inner and outer borders of the inner nuclear layer (INL), although fluorescein angiography (FA) has shown a two-dimensional vascular picture.[7,8] Most OCTA machines and their software for image analyses allow individual evaluations of the superficial and deep capillary plexuses, which contain vessels in the NFL and GCL, or those in the inner and outer borders of the INL in chorioretinal diseases.[9–16] The capillaries in the FA images correspond approximately to those in the superficial layer on OCTA images, which suggests that a systematic evaluation of both the superficial and deep capillary layers would lead to a better understanding of the NPAs in DR.[17] Despite the great advantage of OCTA imaging, we have to consider that the segmentation error or edematous changes did not allow correct evaluation on the en face images constructed according to the default setting, and capillaries should be evaluated three-dimensionally.

Optical coherence tomography (OCT) has visualized morphologic changes in the neuroglial components in diabetic retinas.[18] Cystoid macular edema (CME) and serous retinal detachments (SRDs) were reported first as typical neuronal lesions in DME.[19] A honeycomb pattern or petalloid pattern hyperfluorescence corresponds to cystoid spaces in the INL and Henle's fiber layer (HFL) on OCT images, and foveal cystoid spaces are accompanied by an enlarged foveal avascular zone (FAZ) in DME.[20,21] Other biomarkers of clinical relevance, the external limiting membrane and the ellipsoid zone of the photoreceptors (EZ), represent the integrity of the outer retinal layers, whereas disorganization of the retinal inner layers (DRIL) at the fovea also is related to visual function.[22–25]

The relationship between FA and OCT elucidated that the boundary between the NFL and GCL/inner plexiform layer

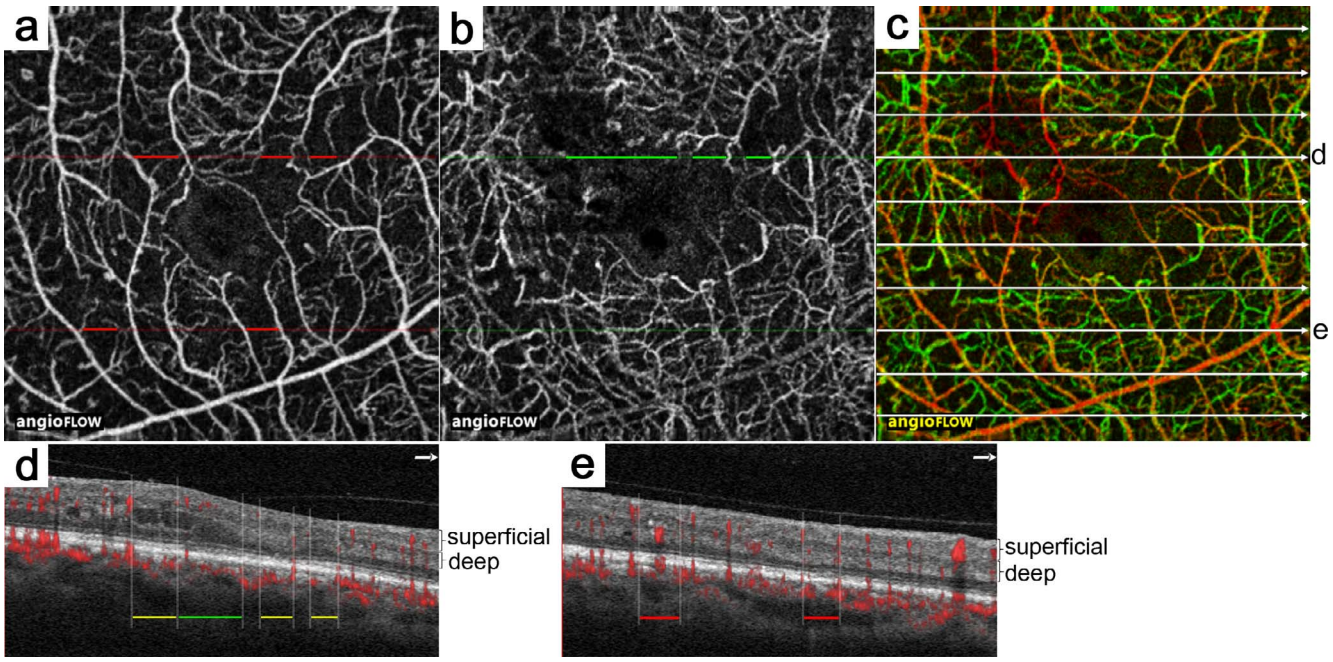

FIGURE 1. The nonperfused areas (NPAs) in the superficial layer, deep layer, and both layers (sNPA, dNPA, and bNPA, respectively) in diabetic retinopathy. En face optical coherence tomography angiography images in the superficial layer (**a**) and the deep layer (**b**). *Dark red and green lines* indicate the nonperfused areas in superficial and deep layers along the fourth or eighth line in (**c**). (**c**) The merged image (*red*: superficial; *green*: deep). In this study, OCTA and structural OCT images along 10 *white arrows* were evaluated. (**d**) The bNPA (*yellow lines*) and dNPA (*green line*) were shown in the retinal sectional image along the fourth line in (**c**). (**e**) The sNPA (*red lines*) on the B-scan image along the eighth line in (**c**).

(IPL) is often indistinct in the NPAs on FA images.[26] En face OCT images delineate inner retinal spots with lower OCT reflectivity in the NFL and higher reflectivity in the GCL, referred to as inner retinal spots with inverted OCT reflectivity, most of which are seen in the hypofluorescent areas.[27] However, it is largely unknown how the lamellar capillary nonperfusion contributes to the development or progression of these neuroglial lesions and concomitant visual impairment in DR.

The current study investigated the relationship between lamellar capillary nonperfusion and corresponding structural changes in the neuroglial components in DR using three-dimensional OCTA and OCT images.

METHODS

Patients

We retrospectively reviewed 101 consecutive eyes of 69 patients with DR who visited the Department of Ophthalmology of Kyoto University Hospital from March 2015 to November 2016. The inclusion criterion was the availability of OCTA images of sufficient quality obtained using Optovue RTVue XR Avanti (Optovue, Inc., Freemont, CA, USA). The exclusion criteria were the presence of other chorioretinal diseases; glaucoma or ocular hypertension; optic nerve diseases including ischemic optic neuropathy; a history of any intervention for macular lesions; intraocular surgery other than cataract surgery; and cataract surgery within 6 months of study enrollment. We further excluded eyes with a displacement artifact, which corresponds to the discontinuity along the B-scan direction caused by eye motion during the raster scan, or a signal strength index (SSI) score of 60 or less to guarantee image quality.[28] Thirty eyes had center-involved DME, which was determined by two-dimensional mapping using the Optovue RTVue XR Avanti as described recently.[29]

All research and measurements adhered to the tenets of the Declaration of Helsinki. The ethics committee of Kyoto University Graduate School and Faculty of Medicine approved the study protocol. All participants provided written informed consent before study entry.

Optical Coherence Tomography Angiography

After a comprehensive ophthalmic examination, retinal specialists evaluated fundus findings, and we reviewed the international grades of DR severity from medical records. OCTA and OCT images of the 3 × 3-mm square (corresponding to 304 × 304 pixels) centered on the fovea were obtained simultaneously and coregistered using the Optovue RTVue XR Avanti (Fig. 1). This instrument enables acquisition of reflectivity signals at a high A-scan rate of 70,000 scans/second using a light source of approximately 840 nm; the split-spectrum amplitude decorrelation angiography algorithm demonstrates motion-dependent angiography as described previously.[5] Two consecutive B-scans were acquired at a fixed position before proceeding to the next position. After processing the volume scans, the calculation of the signal decorrelation between the sequential images leads to detection of erythrocyte motion and resultant construction of a motion contrast "angioflow" image.

We then evaluated the NPAs in the superficial or deep layers (sNPA and dNPA, respectively) on the OCTA images. The perfusion status along 10 of 304 transverse lines (5th, 35th, 65th, 95th, 125th, 155th, 185th, 215th, 245th, and 275th lines from the most superior line) was estimated three-dimensionally using both en face and sectional images of the decorrelation signals (Fig. 1). We first screened the sNPA or dNPA using the en face images in the superficial layer (slab images from the inner boundary 3 μm beneath the internal limiting membrane to the outer boundary 15 μm beneath the IPL) and the deep layer (slab images from the inner boundary 15 μm beneath the IPL to the outer boundary 70 μm beneath the IPL), according

to the default setting of the manufacturer's software (Optovue, Inc.). We then confirmed the absence of decorrelation signals in the corresponding layers on the B-scan images. Retinal capillaries are mainly in the NFL, GCL, and the inner and outer borders of the INL.[7,8] The superficial layer contains most of the capillary plexuses in the NFL and GCL/IPL, whereas two capillary layers in the INL are in the deep layer. We determined the sNPAs as the areas without decorrelation signals in the NFL or GCL/IPL alone on B-scan images. Similarly, the dNPAs were defined as the areas without decorrelation signals in the INL alone. The NPAs in both the superficial and deep capillary layers were referred to as the bNPA in this study. Two masked retina specialists measured the transverse length of the sNPA, dNPA, or bNPA along 10 horizontal lines, and the averages of the measurements were used for further investigation. Briefly, the B-scan images with the decorrelation signals were exported into ImageJ software (National Institutes of Health, Bethesda, MD, USA). The straight line tool and the following measure function were applied to count the horizontal pixel number, which was converted to the transverse length.

Optical Coherence Tomography

We evaluated the structural changes in the neuroglial tissues corresponding to the NPA in individual layers, that is, areas with no boundary between the NFL and GCL/IPL, inner retinal spots with inverted OCT reflectivity, and cystoid spaces in the INL and HFL.[20,26,27] The transverse lengths of these lesions were individually quantified using the ImageJ software as described above. The OCT reflectivity of the NFL is much higher than that of the GCL/IPL on B-scan images in healthy eyes, which enabled identification of the boundary between these layers. In contrast, the boundary is often indistinct in the areas with a NPA on FA images in diabetic eyes, whose transverse length was measured.[26]

Another OCT finding in the inner retinal layers, the spot with inverted reflectivity on OCT images using the Optovue RTVue XR Avanti, also was evaluated according to modified methods as described previously.[27] We sometimes found well-defined spots with lower reflectivity in the NFL and higher reflectivity in the GCL/IPL in the sNPA, after the en face OCT images in the NFL or GCL were constructed using the manual setting of the inner and outer borders of these layers in the localized areas. When the boundary between the GCL and IPL was indefinite, we constructed en face images from the inner border of the GCL to the center of the GCL/IPL to evaluate the patchy lesions in the GCL. We determined such lesions using en face and B-scan images and measured the transverse length of these lesions in the NFL along the 10 lines on the B-scan images. Cotton-wool spots are structural changes in focal NPAs. However, we did not evaluate these lesions, which were observed mainly around the vascular arcade but rarely within the central 3 × 3-mm square.

We also individually quantified the transverse length of the areas with cystoid spaces in the INL and HFL.[20] Cystoid spaces in the fovea, where inner retinal layers were absent, were allocated to those in the HFL. Most cystoid spaces were delineated in either the INL or HFL, although we rarely observed enlarged cystoid spaces extending from the INL to the HFL.[24] The areas with such lesions were counted as cystoid spaces in the INL and HFL.

Statistical Analysis

The results are expressed as the median (interquartile range, IQR). The agreement of qualitative parameters measured by two retina specialists was confirmed using the intraclass correlation coefficients (ICCs). The data were analyzed using the Mann-Whitney *U* test or Kruskal-Wallis test with Bonferroni correction to evaluate the differences among groups. The sampling distribution was evaluated using Fisher's exact test. Spearman's correlation coefficient was calculated to test the statistical correlation. $P < 0.05$ was considered significant.

Table. Patients' Characteristics

Parameter	
Eyes/patients	101/69
Age, y, median (IQR)	66 (53 to 71)
Sex	
Men	57
Women	12
Hemoglobin A1c, %, median (IQR)	7.8 (6.6 to 8.5)
Systemic hypertension	
Absent	33
Present	36
logMAR VA, median (IQR)	0.000 (−0.079 to 0.097)
Lens status	
Phakia	81 eyes
Pseudophakia	20 eyes
DR severity	
Moderate NPDR	58 eyes
Severe NPDR	13 eyes
PDR	30 eyes
Panretinal photocoagulation	
Absent	70 eyes
Present	31 eyes
CSF thickness, μm, median (IQR)	285 (255 to 332)

logMAR VA, logarithm of the minimum angle of resolution visual acuity; NPDR, nonproliferative diabetic retinopathy; PDR, proliferative diabetic retinopathy; CSF, central subfield.

Results

Three Patterns of Lamellar Capillary Nonperfusion

After we excluded 45 eyes with poor-quality OCTA images, we retrospectively reviewed 101 eyes of 69 patients with DR, whose characteristics are shown in the Table. The sNPA, dNPA, and bNPA were delineated along 10 horizontal lines (30 mm in total length) within a 3 × 3-mm square centered on the fovea in 87, 56, and 101 eyes, respectively (ICCs, 0.962, 0.975, and 0.986, respectively; Fig. 1). The transverse lengths of the sNPA and dNPA were 0.703 mm (0.244–1.664) and 0.184 mm (0–0.598), respectively (2.34% [0.81–5.55] and 0.61% [0–1.99]) (Fig. 2a). The length of the bNPA was 1.789 mm (1.206–3.264) (5.96% [4.02–10.88]). The transverse length of the sNPA was correlated modestly ($\rho = 0.366$, $P < 0.001$) with that of the bNPA (Fig. 2b), whereas the dNPA was not associated with the bNPA or sNPA (Figs. 2c, 2d).

We compared the transverse lengths of the NPAs in eyes with center-involved DME to those in eyes without DME. Thirty eyes with DME had longer transverse length of the dNPA than 71 eyes without DME (0 mm [0–0.368] vs. 0.518 mm [0.150–1.196], $P < 0.001$). By contrast, there were no differences in the transverse length of the bNPA or sNPA between eyes with and without DME ($P = 0.704$ or $P = 0.493$, respectively).

Structural Changes in the Neuroglial Tissue in Areas of Lamellar Capillary Nonperfusion

We investigated how lamellar capillary nonperfusion is associated with the structural changes in the neuroglial tissues

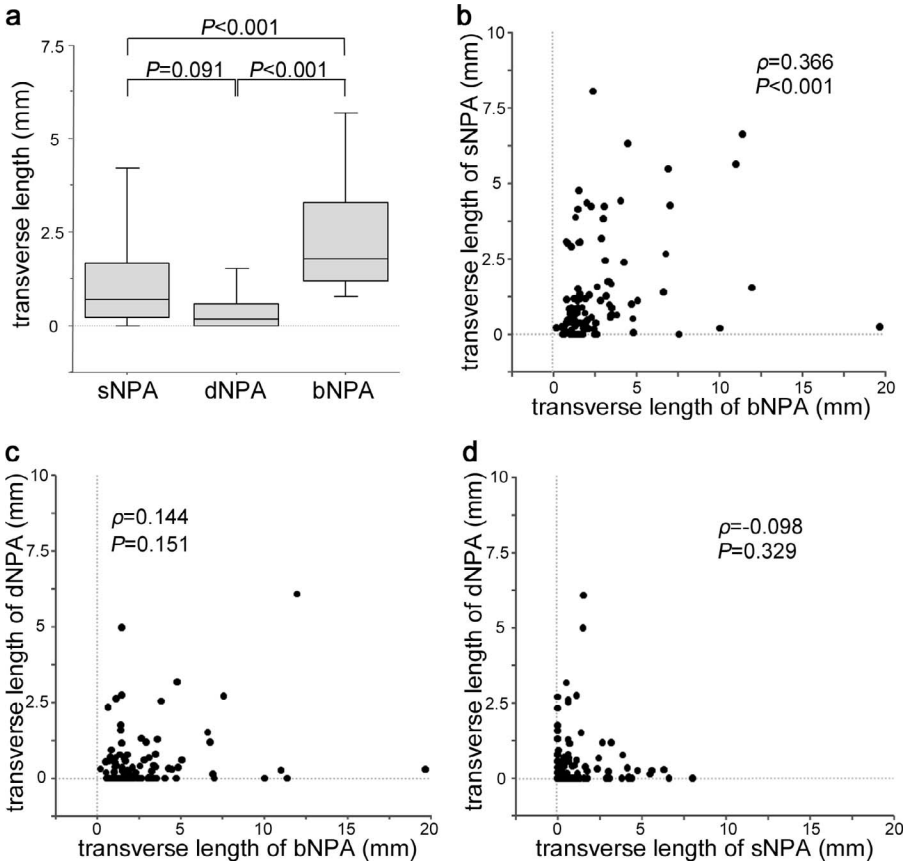

Figure 2. The transverse length of the nonperfused areas (NPAs) in the superficial capillary plexus, deep capillary plexus, and both plexuses (sNPA, dNPA, and bNPA, respectively) in diabetic retinopathy. (**a**) The transverse length of individual patterns of NPAs. (**b**, **c**) The association of the transverse length of the bNPA with those of the sNPA and dNPA. (**d**) The relationship between the lengths of sNPA and the dNPA.

on the OCT sectional images. The areas with no boundary between the NFL and GCL/IPL, which included the foveal center, were observed and quantified in all 101 eyes (ICC, 0.918; Figs. 3, 4). The proportion of the horizontal length of this OCT finding in the sNPA, dNPA, and bNPA was significantly ($P < 0.001$ for all comparisons) higher than that in the perfused area (PA) (Fig. 5a). The transverse lengths of the sNPA, dNPA, and bNPA also were correlated significantly with the length of no boundary between the NFL and GCL/IPL in the corresponding NPAs ($\rho = 0.836$, $P < 0.001$, $\rho = 0.747$, $P < 0.001$, and $\rho = 0.865$, $P < 0.001$, respectively; Figs. 6a, 6d, 6g).

Inner retinal spots with inverted OCT reflectivity were seen and measured in 48 eyes (ICC, 0.948; Fig. 7). The percentages of the transverse lengths of such spots in the sNPA were significantly ($P < 0.001$ for all comparisons) higher than in the PA, dNPA, and bNPA (Fig. 5b). A significant correlation also was seen between the transverse length of the sNPA and this OCT finding within the sNPA ($\rho = 0.519$, $P < 0.001$; Fig. 6b). Cotton-wool spots correspond to the focal ischemia around the vascular arcades in the FA images, whereas we rarely found them in the central 3 × 3-mm square.

Cystoid spaces, a major finding in the middle or outer retinal layers, are mainly in the INL and HFL and were seen in the INL in 38 eyes (Fig. 8). Twenty-two eyes (57.9%) with cystoid spaces in the INL had center-involved DME, whereas only 8 (12.7%) of 63 eyes without such cystoid spaces were accompanied by DME ($P < 0.001$). We then quantified the transverse length of cystoid spaces in the INL or HFL (ICC, 0.961 and 0.972, respectively), and compared such lesions to the NPAs. The proportion of horizontal length of cystoid spaces in the INL was significantly higher in the dNPA than in the PA, sNPA, and bNPA ($P < 0.001$, $P = 0.011$, and $P = 0.014$, respectively; Fig. 5c). The length of the dNPA was correlated significantly with that of the cystoid spaces in the INL in the dNPA ($\rho = 0.770$, $P < 0.001$; Fig. 6e). Fifty-eight eyes had cystoid spaces in the HFL, and the proportion of horizontal length of cystoid spaces in the HFL was significantly higher in the dNPA and bNPA than in the PA ($P = 0.004$ and $P < 0.001$, respectively; Fig. 5d). The length of the dNPA was correlated significantly with that of the cystoid spaces in the HFL in the dNPA ($\rho = 0.757$, $P < 0.001$; Fig. 6f), compared to no association in the bNPA ($\rho = 0.256$, $P = 0.053$; Fig. 6i).

Discussion

In addition to vascular hyperpermeability, capillary nonperfusion leads to dysfunction of the neuroglial components in DR. The development of OCTA technology has enabled noninvasive appreciation of the three-dimensional structure of the retinal vasculature in DR, whereas FA, the invasive classical modality, provides only two-dimensional fluorescent signals derived mainly from the superficial retinal layers.[9,10,17,30] The current study showed the systematic relationship between the lamellar capillary nonperfusion on OCTA images and structural changes in the corresponding neuroglial components in the OCT images. Intriguingly, the sNPA had inner retinal lesions, that is, inner retinal spots with inverted OCT reflectivity and no boundary between the NFL and GCL/IPL.[26,27] The dNPA was accompanied frequently not only by neuroglial changes in the

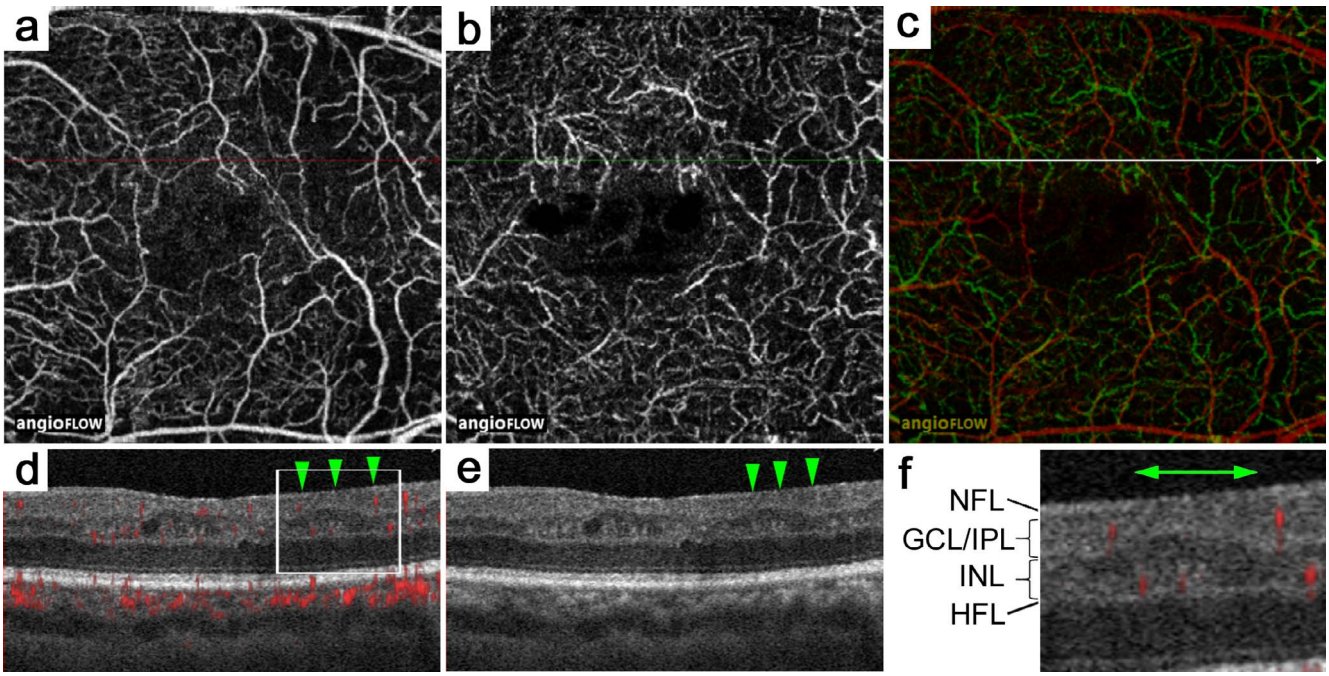

FIGURE 3. No boundary between the nerve fiber layer (NFL) and ganglion cell layer/inner plexiform layer (GCL/IPL) within the nonperfused area in the superficial layer (sNPA) in a 68-year-old patient with proliferative diabetic retinopathy. En face optical coherence tomography angiography images of the superficial layer (**a**), the deep layer (**b**), and the merged image (**c**) (*red*: superficial, *green*: deep). (**d**, **e**) The sectional images with and without a decorrelation signal along the arrow in (**a**–**c**) show the absence of a boundary between the NFL and GCL/IPL within the sNPA (*arrowheads*). (**f**) A magnified image of the *square* in (**d**). The *double-headed arrow* indicates the area with no boundary between the NFL and GCL/IPL.

corresponding layer, that is, cystoid spaces, but also by morphologic changes in other layers. These data suggested the clinical feasibility of a three-dimensional evaluation of the disruption in the neurovascular units in DR. Previous publications demonstrated the relationship between retinal dysfunction and circulatory disturbance on FA images, which may be consistent with the structural changes in the lamellar NPAs on OCTA images in this study.[31,32] Further investigation

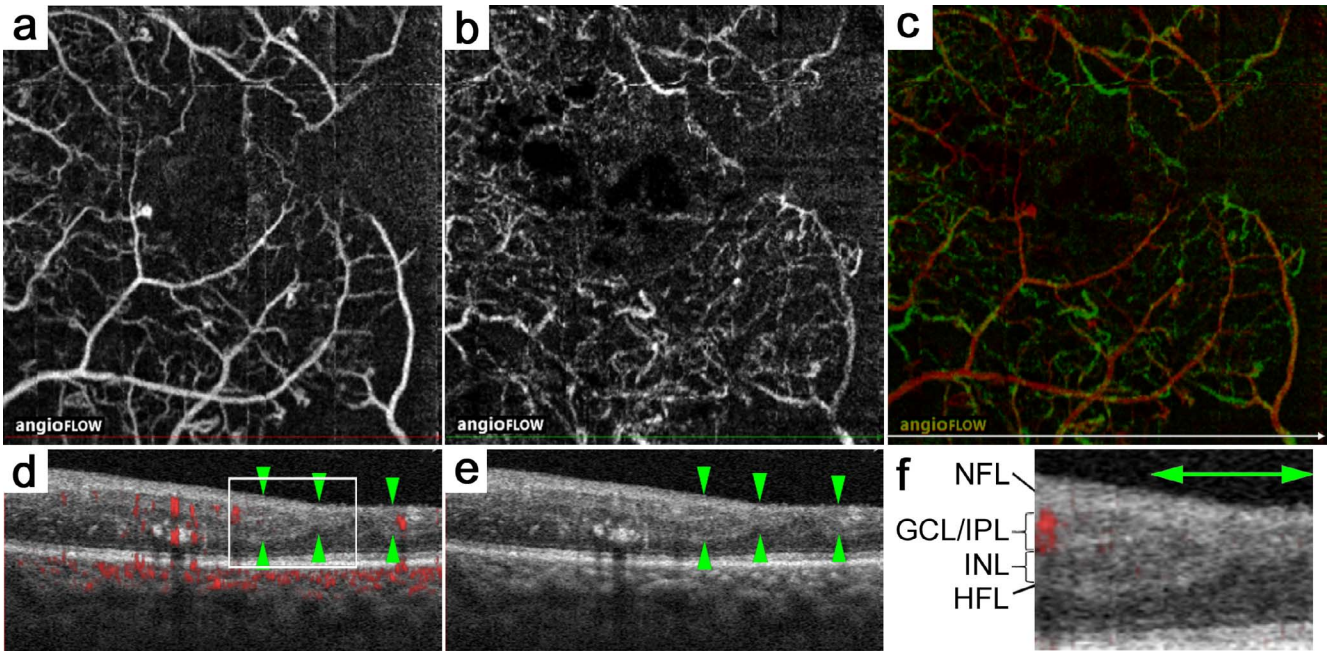

FIGURE 4. No boundary between the nerve fiber layer (NFL) and ganglion cell layer/inner plexiform layer (GCL/IPL) within the nonperfused area in both the superficial and deep layers (bNPA) in a 42-year-old patient with proliferative diabetic retinopathy. En face optical coherence tomography angiography images in the superficial layer (**a**), the deep layer (**b**), and the merged image (**c**) (*red*: superficial, *green*: deep). (**d**, **e**) The sectional images with and without a decorrelation signal along the *arrow* in (**a**–**c**) show the absence of a boundary between the NFL and GCL/IPL within the bNPA (*arrowheads*). (**f**) A magnified image of the *square* in (**d**). The *double-headed arrows* indicate the areas with no boundary between the NFL and GCL/IPL.

Investigative Ophthalmology & Visual Science

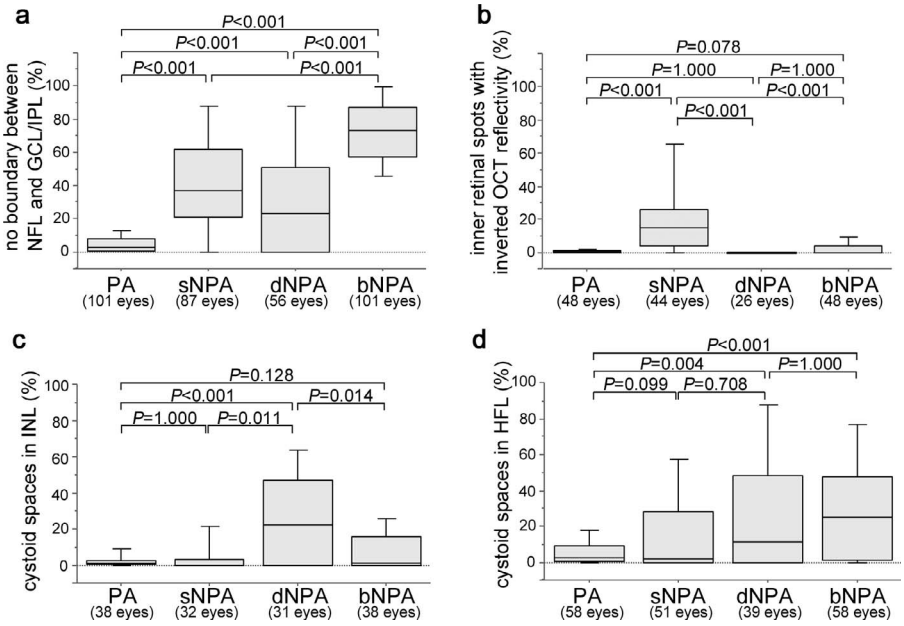

Figure 5. The transverse length of neuroglial findings in the lamellar nonperfused areas (NPAs) in diabetic retinopathy. (**a**) The percentage of the transverse length of the areas with no boundary between the nerve fiber layer (NFL) and ganglion cell layer/inner plexiform layer (GCL/IPL) within the perfused area (PA), the nonperfused area in the superficial layer (sNPA), the deep layer (dNPA), or both layers (bNPA) to the length of the areas with the corresponding perfusion status. (**b**) The percentage of the length of the inner retinal spots with inverted optical coherence tomography (OCT) reflectivity, (**c**) cystoid spaces in the inner nuclear layer (INL), and (**d**) those in the Henle's fiber layer (HFL) in the areas with individual perfusion status.

should elucidate the association between the dysfunction and lamellar changes in neurovascular units in DR.

Before interpreting the current data, we have to point out the limitations regarding the retinal vasculature seen in the OCTA images. The decorrelation signals can delineate the vasculature with limited velocity of the blood flow.[33] In addition, the movement of the erythrocytes is unstable in diabetic retinas, and inconsistencies often are seen between the structure and function of the retinal vessels. For example, the decorrelation signals in the microaneurysms can appear or disappear in sequentially acquired images, and the redelineation of the decorrelation signals in the NPA represents the reperfusion.[28,34] We thus speculated that the NPAs in the OCTA images correspond to either complete loss of the capillary beds or reduced velocity of the erythrocyte movement. In addition, the projection artifacts in hyperreflective lesions or segmentation error and shadow artifacts in retina edema do not enable OCTA to depict retinal vascular structure exactly.

A recent study reported an OCT finding in the NPA on FA images, that is, no boundary between the NFL and GCL/IPL, which is consistent with such lesions in the bNPA on OCTA images.[26] Intriguingly, we also observed no boundary between these layers within the sNPA. A novel OCT finding, the inner retinal spots with inverted OCT reflectivity, also was seen in the sNPA.[27] Since the capillaries in the superficial layer are mainly in the NFL and GCL, the lamellar ischemia in these layers might promote structural disruption in the corresponding layers.[7,8,14] In contrast, diabetes induces neurodegeneration in the NFL and GCL, which might reduce the vasculogenic factors and subsequent loss of capillaries.[35–38] We speculated that the differences in the size and morphologies between these OCT lesions in the sNPA might depend on different mechanisms. Further investigation should elucidate the pathologic mechanisms and visual impairments regarding these lesions.

We showed the association between the dNPA and cystoid spaces in the INL. Since capillaries in the deep layer reside mainly in the inner and outer borders of the INL, the lamellar ischemia in the middle layers might disrupt the exchanges in oxygen, nutrients, and wastes and concomitant accumulation of intracytoplasmic or extracellular fluids.[39–41] Vascular hyperpermeability might result in development of cystoid spaces in the INL, which subsequently might compress the surrounding vessels and reduce the velocity or amount of blood flow. In contrast, capillary loss in the deep layer might disrupt the pump function in the Müller cells or drainage of the extravascular fluids from the capillaries there, which might lead to edematous changes in the neuroglial components. We had to consider that the dNPA around the cystoid spaces might be an artifact, a flow void, although we carefully evaluated the decorrelation signals in both the en face and B-scan images.[28] A recent study documented paracentral acute middle maculopathy, in which the retinal arteries were occluded in the middle layer and the parenchyma was accompanied by higher OCT reflectivity rather than cystoid spaces in the INL.[42] The mechanisms in these diseases might be different, transient or persistent obstruction, vessel-to-neuron or neuron-to-vessel changes. It remains to be seen what determines the differences between these OCT lesions corresponding to the circulatory disturbance in the INL.

We also found an association between the dNPA and two OCT findings in other retinal layers, that is, no boundary between the NFL and GCL/IPL and cystoid spaces in the HFL. The dNPA might promote the degenerative changes in the bipolar cells and the dysfunction of the Müller cells. The anterograde degeneration or insufficient metabolism in the Müller cells might contribute to ganglion cell loss. The retrograde degeneration also might exacerbate the photoreceptor damage with concomitant disruption of the EZ lines or cystoid spaces in the HFL.[43,44] Another possibility is that the capillary loss in the deep layer might reduce the drainage of extracellular fluids and thereby increase the extracellular fluids

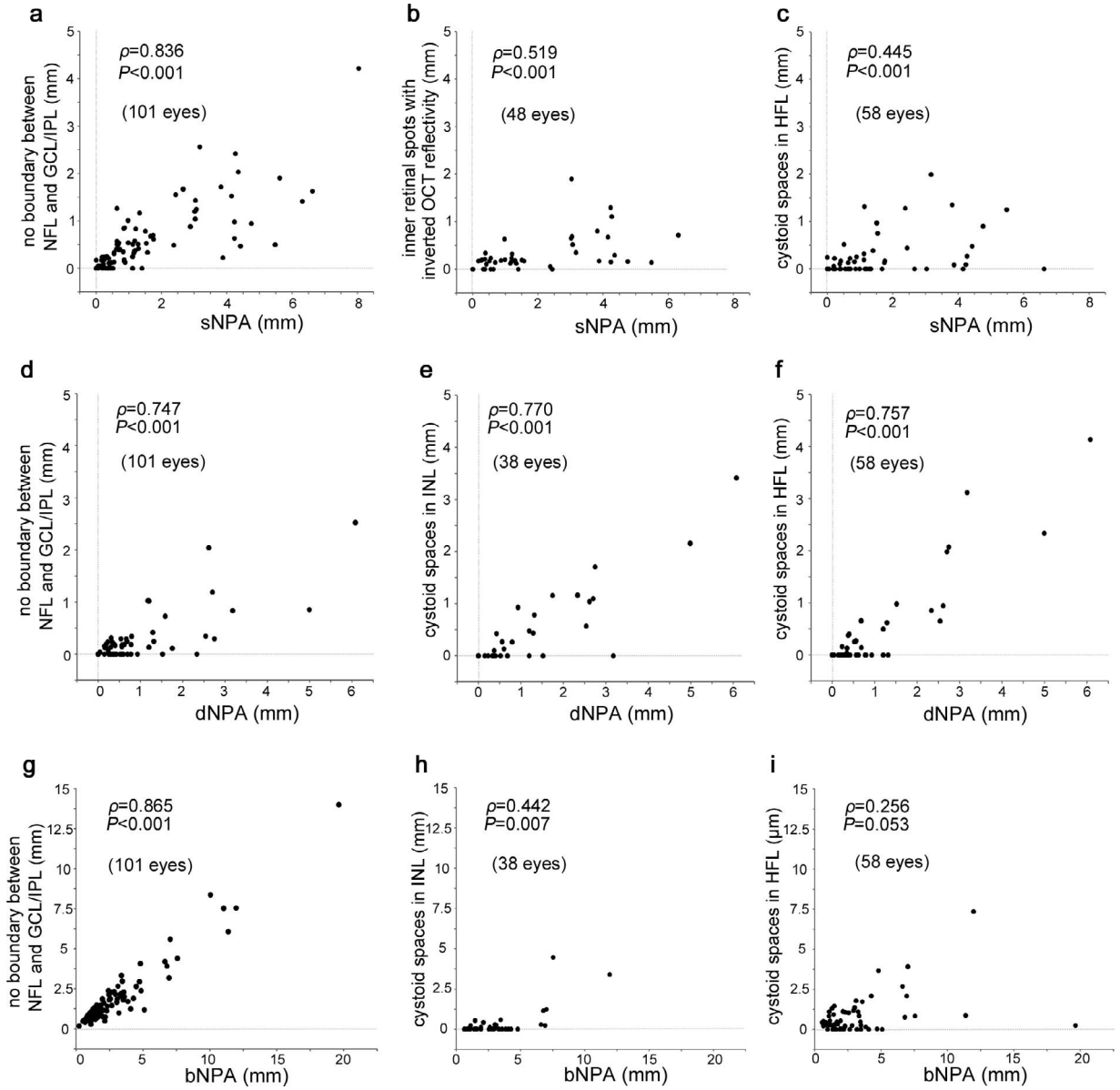

Figure 6. Association between the transverse lengths of neuroglial findings and the lamellar nonperfused areas (NPAs) in diabetic retinopathy. (**a**–**c**) The association between the transverse lengths of the NPA in the superficial layer (sNPA) and individual neuroglial findings in the sNPA. (**d**–**f**) The correlation between the transverse length of the NPA in the deep layer (dNPA) and individual neuroglial findings in the dNPA. (**g**–**i**) The relationship between the transverse length of the NPAs in both layers (bNPA) and individual neuroglial findings in the bNPA.

in the HFL, as discussed regarding the cystoid spaces in the INL.

In the current study, center-involved DME was associated with both the dNPA and cystoid spaces in the INL. We might hypothesize that the dNPA in the parafovea contributes to the pathogenesis in both such cystoid spaces in the corresponding areas and retinal thickening in the fovea. The imbalance between the diapedesis and absorption of extracellular fluids in the extrafoveal areas might promote foveal SRD.[45] Foveal cystoid spaces are often accompanied by the larger FAZ, which may be consistent with the association between the dNPA and cystoid spaces in the INL in the parafovea.[21]

The current study, which focused on the structural changes in the retinal layers corresponding to the sNPA or dNPA, had several limitations. Further investigations should determine the relationship between lamellar ischemia and other OCT findings between layers, for example, DRIL, extended cystoid spaces, or SRD.[19,24,25] The areas without capillaries were composed of both normal FAZ and pathologically developed NPAs around the fovea. Since we could not determine the boundary between them, we included the FAZ in the NPAs in this study. As a result, the NPAs did not always correspond to the pathologic changes. Since OCTA cannot assess vascular permeability, the mechanisms regarding edematous changes including the cystoid spaces are not fully understood. We evaluated the structural changes in the neurovascular components along 10 representative lines in Asian patients with sufficient quality OCTA images in a single center. A future study should evaluate the areas with individual lesions on the two-dimensional plane in larger cohorts to guarantee the generalizability in other institutes in other races.

In conclusion, we showed an association between lamellar capillary nonperfusion and structural changes in the corresponding neuroglial components, which sheds light on the

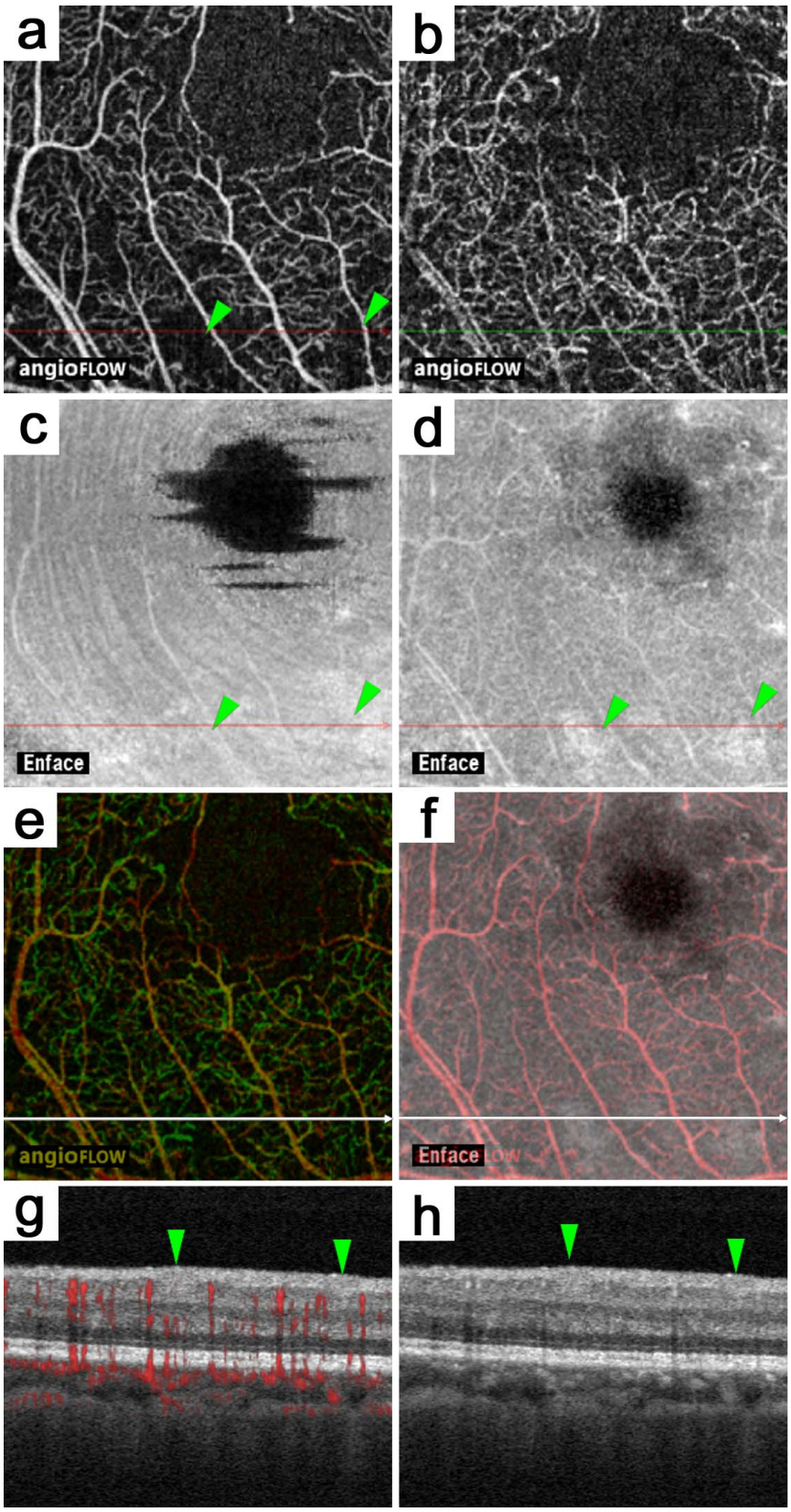

FIGURE 7. Inner retinal spots with inverted reflectivity in the nonperfused area of the superficial layer (sNPA) in a 43-year-old patient with moderate nonproliferative diabetic retinopathy. En face optical coherence tomography (OCT) angiography images in the superficial layer (**a**) and the deep layer (**b**). En face OCT images of the nerve fiber layer (**c**) and the ganglion cell layer (**d**) show the spots with inverted OCT reflectivity (*arrowheads*). (**e**) A merged image of the capillaries in the superficial and deep layers (*red*: superficial, *green*: deep). (**f**) A merged image of (**a**) (*red*) and (**d**) (*grayscale*). (**g**, **h**) A B-scan image with and without a decorrelation signal along the arrow in (**a**–**f**) shows the sectional image of spots with inverted reflectivity in the sNPA (*arrowheads*).

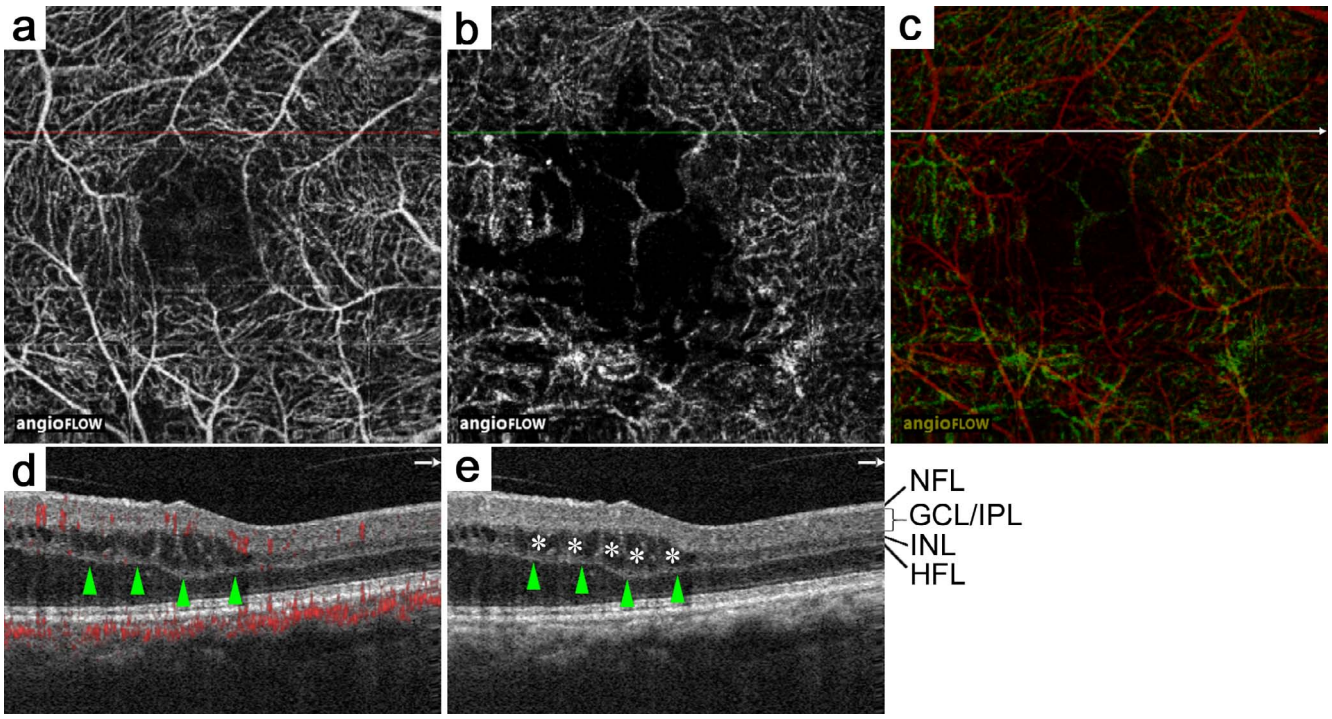

FIGURE 8. Cystoid spaces in the inner nuclear layer (INL) in the nonperfused area of the deep layer (dNPA) in a 66-year-old patient with proliferative diabetic retinopathy. En face optical coherence tomography angiography images in the superficial layer (**a**), the deep layer (**b**), and the merged image (**c**) (*red*: superficial, *green*: deep). (**d**, **e**) Sectional images with and without decorrelation signals along *arrows* in (**a**–**c**) show the cystoid spaces in the INL (*asterisk*) in the dNPA (*arrowheads*).

understanding of the layer-by-layer pathogenesis in the neurovascular units in DR.

Acknowledgments

Supported by a Grant-in-Aid for Scientific Research of the Japan Society for the Promotion of Science (26462637, 17K11423), Japan.

Disclosure: **Y. Dodo**, None; **T. Murakami**, None; **K. Suzuma**, None; **S. Yoshitake**, None; **T. Yoshitake**, None; **K. Ishihara**, None; **M. Fujimoto**, None; **Y. Miwa**, None; **A. Tsujikawa**, None

References

1. Yau JW, Rogers SL, Kawasaki R, et al. Global prevalence and major risk factors of diabetic retinopathy. *Diabetes Care*. 2012;35:556–564.
2. Gardner TW, Antonetti DA, Barber AJ, LaNoue KF, Levison SW. Diabetic retinopathy: more than meets the eye. *Surv Ophthalmol*. 2002;47(suppl 2):S253–S262.
3. Antonetti DA, Klein R, Gardner TW. Diabetic retinopathy. *N Engl J Med*. 2012;366:1227–1239.
4. Mariampillai A, Standish BA, Moriyama EH, et al. Speckle variance detection of microvasculature using swept-source optical coherence tomography. *Opt Lett*. 2008;33:1530–1532.
5. Jia Y, Tan O, Tokayer J, et al. Split-spectrum amplitude-decorrelation angiography with optical coherence tomography. *Opt Express*. 2012;20:4710–4725.
6. Schwartz DM, Fingler J, Kim DY, et al. Phase-variance optical coherence tomography: a technique for noninvasive angiography. *Ophthalmology*. 2014;121:180–187.
7. Gariano RF, Iruela-Arispe ML, Hendrickson AE. Vascular development in primate retina: comparison of laminar plexus formation in monkey and human. *Invest Ophthalmol Vis Sci*. 1994;35:3442–3455.
8. Chan G, Balaratnasingam C, Yu PK, et al. Quantitative morphometry of perifoveal capillary networks in the human retina. *Invest Ophthalmol Vis Sci*. 2012;53:5502–5514.
9. Takase N, Nozaki M, Kato A, Ozeki H, Yoshida M, Ogura Y. Enlargement of foveal avascular zone in diabetic eyes evaluated by en face optical coherence tomography angiography. *Retina*. 2015;35:2377–2383.
10. Ishibazawa A, Nagaoka T, Takahashi A, et al. Optical coherence tomography angiography in diabetic retinopathy: a prospective pilot study. *Am J Ophthalmol*. 2015;160:35–44.e1.
11. Balaratnasingam C, Inoue M, Ahn S, et al. Visual acuity is correlated with the area of the foveal avascular zone in diabetic retinopathy and retinal vein occlusion. *Ophthalmology*. 2016;123:2352–2367.
12. Lee J, Moon BG, Cho AR, Yoon YH. Optical coherence tomography angiography of DME and its association with anti-VEGF treatment response. *Ophthalmology*. 2016;123:2368–2375.
13. Samara WA, Shahlaee A, Adam MK, et al. Quantification of diabetic macular ischemia using optical coherence tomography angiography and its relationship with visual acuity. *Ophthalmology*. 2017;124:235–244.
14. Snodderly DM, Weinhaus RS, Choi JC. Neural-vascular relationships in central retina of macaque monkeys (Macaca fascicularis). *J Neurosci*. 1992;12:1169–1193.
15. Hwang TS, Zhang M, Bhavsar K, et al. Visualization of 3 distinct retinal plexuses by projection-resolved optical coherence tomography angiography in diabetic retinopathy. *JAMA Ophthalmol*. 2016;134:1411–1419.
16. Salz DA, de Carlo TE, Adhi M, et al. Select features of diabetic retinopathy on swept-source optical coherence tomographic angiography compared with fluorescein angiography and normal eyes. *JAMA Ophthalmol*. 2016;134:644–650.

17. Spaide RF, Klancnik JM Jr, Cooney MJ. Retinal vascular layers imaged by fluorescein angiography and optical coherence tomography angiography. *JAMA Ophthalmol*. 2015;133:45–50.
18. Murakami T, Yoshimura N. Structural changes in individual retinal layers in diabetic macular edema. *J Diabetes Res*. 2013; 2013:920713.
19. Otani T, Kishi S, Maruyama Y. Patterns of diabetic macular edema with optical coherence tomography. *Am J Ophthalmol*. 1999;127:688–693.
20. Otani T, Kishi S. Correlation between optical coherence tomography and fluorescein angiography findings in diabetic macular edema. *Ophthalmology*. 2007;114:104–107.
21. Murakami T, Nishijima K, Sakamoto A, Ota M, Horii T, Yoshimura N. Foveal cystoid spaces are associated with enlarged foveal avascular zone and microaneurysms in diabetic macular edema. *Ophthalmology*. 2011;118:359–367.
22. Sakamoto A, Nishijima K, Kita M, Oh H, Tsujikawa A, Yoshimura N. Association between foveal photoreceptor status and visual acuity after resolution of diabetic macular edema by pars plana vitrectomy. *Graefes Arch Clin Exp Ophthalmol*. 2009;247:1325–1330.
23. Murakami T, Nishijima K, Sakamoto A, Ota M, Horii T, Yoshimura N. Association of pathomorphology, photoreceptor status, and retinal thickness with visual acuity in diabetic retinopathy. *Am J Ophthalmol*. 2011;151:310–317.
24. Murakami T, Nishijima K, Akagi T, et al. Optical coherence tomographic reflectivity of photoreceptors beneath cystoid spaces in diabetic macular edema. *Invest Ophthalmol Vis Sci*. 2012;53:1506–1511.
25. Sun JK, Lin MM, Lammer J, et al. Disorganization of the retinal inner layers as a predictor of visual acuity in eyes with center-involved diabetic macular edema. *JAMA Ophthalmol*. 2014; 132:1309–1316.
26. Dodo Y, Murakami T, Uji A, Yoshitake S, Yoshimura N. Disorganized retinal lamellar structures in nonperfused areas of diabetic retinopathy. *Invest Ophthalmol Vis Sci*. 2015;56: 2012–2020.
27. Yoza R, Murakami T, Uji A, et al. Characterization of inner retinal spots with inverted reflectivity on en face optical coherence tomography in diabetic retinopathy. *Invest Ophthalmol Vis Sci*. 2016;57:1862–1870.
28. Spaide RF, Fujimoto JG, Waheed NK. Image artifacts in optical coherence tomography angiography. *Retina*. 2015;35:2163–2180.
29. Bressler SB, Edwards AR, Andreoli CM, et al. Reproducibility of Optovue RTVue optical coherence tomography retinal thickness measurements and conversion to equivalent Zeiss Stratus metrics in diabetic macular edema. *Trans Vis Sci Tech*. 2015;4(1):5.
30. Spaide RF. Volume-rendered angiographic and structural optical coherence tomography. *Retina*. 2015;35:2181–2187.
31. Arend O, Wolf S, Jung F, et al. Retinal microcirculation in patients with diabetes mellitus: dynamic and morphological analysis of perifoveal capillary network. *Br J Ophthalmol*. 1991;75:514–518.
32. Arend O, Remky A, Evans D, Stuber R, Harris A. Contrast sensitivity loss is coupled with capillary dropout in patients with diabetes. *Invest Ophthalmol Vis Sci*. 1997;38:1819–1824.
33. Ploner SB, Moult EM, Choi W, et al. Toward quantitative optical coherence tomography angiography: visualizing blood flow speeds in ocular pathology using variable interscan time analysis. *Retina*. 2016;36(suppl 1):S118–S126.
34. Miwa Y, Murakami T, Suzuma K, et al. Relationship between functional and structural changes in diabetic vessels in optical coherence tomography angiography. *Sci Rep*. 2016;6:29064.
35. Chihara E, Matsuoka T, Ogura Y, Matsumura M. Retinal nerve fiber layer defect as an early manifestation of diabetic retinopathy. *Ophthalmology*. 1993;100:1147–1151.
36. Barber AJ, Lieth E, Khin SA, Antonetti DA, Buchanan AG, Gardner TW. Neural apoptosis in the retina during experimental and human diabetes. Early onset and effect of insulin. *J Clin Invest*. 1998;102:783–791.
37. Gastinger MJ, Kunselman AR, Conboy EE, Bronson SK, Barber AJ. Dendrite remodeling and other abnormalities in the retinal ganglion cells of Ins2 Akita diabetic mice. *Invest Ophthalmol Vis Sci*. 2008;49:2635–2642.
38. Kim I, Ryan AM, Rohan R, et al. Constitutive expression of VEGF, VEGFR-1, and VEGFR-2 in normal eyes. *Invest Ophthalmol Vis Sci*. 1999;40:2115–2121.
39. Yanoff M, Fine BS, Brucker AJ, Eagle RC Jr. Pathology of human cystoid macular edema. *Surv Ophthalmol*. 1984; 28(suppl):505–511.
40. Fine BS, Brucker AJ. Macular edema and cystoid macular edema. *Am J Ophthalmol*. 1981;92:466–481.
41. Tso MO. Pathology of cystoid macular edema. *Ophthalmology*. 1982;89:902–915.
42. Sarraf D, Rahimy E, Fawzi AA, et al. Paracentral acute middle maculopathy: a new variant of acute macular neuroretinopathy associated with retinal capillary ischemia. *JAMA Ophthalmol*. 2013;131:1275–1287.
43. Scarinci F, Nesper PL, Fawzi AA. Deep retinal capillary nonperfusion is associated with photoreceptor disruption in diabetic macular ischemia. *Am J Ophthalmol*. 2016;168:129–138.
44. Spaide RF. Retinal vascular cystoid macular edema: review and new theory. *Retina*. 2016;36:1823–1842.
45. Murakami T, Uji A, Ogino K, et al. Association between perifoveal hyperfluorescence and serous retinal detachment in diabetic macular edema. *Ophthalmology*. 2013;120:2596–2603.

Investigative Ophthalmology & Visual Science